CHEMISTRY OF MATERIALS

COMMUNICATION

pubs.acs.org/cm

# Epitaxial Electrodeposition of $Fe_3O_4$ on Single-Crystal Ni(111)

Rakesh V. Gudavarthy,[†] Sandeep Gorantla,[‡] Guojun Mu,[†] Elizabeth A. Kulp,[†] Thomas Gemming,[‡] Jürgen Eckert,[‡] and Jay A. Switzer*[,†]

[†]Department of Chemistry and Graduate Center for Materials Research, Missouri University of Science and Technology, Rolla, Missouri 65409-1170, United States

[‡]IFW Dresden, Institute for Complex Materials, P.O. Box 270116, D-01171 Dresden, Germany

**KEYWORDS:** epitaxy, electrodeposition, magnetite, resistance switching

Magnetite, $Fe_3O_4$, is a promising source of spin polarized carriers. Being a half-metallic material with 100% spin polarization at the Fermi level,[1] $Fe_3O_4$ is a good candidate for spin-based devices such as magnetic random access memory (MRAM), magnetic heads, and magnetic sensors.[2] A large magnetoresistance effect has been reported for $Fe_3O_4$ nanostructures, tunnel junctions, and grain boundaries.[3] Epitaxial growth of $Fe_3O_4$ has been demonstrated by several groups and interesting magnetic properties such as superparamagnetism,[4] slow saturation behavior,[5] and local out-of-plane magnetic moments in zero field[5] have been observed. The $Fe_3O_4$/Ni epitaxial system is interesting because of the large lattice mismatch, because of the question of whether the $Fe_3O_4$ grows directly on Ni(111) or is separated by a thin NiO layer, and because of possible applications for spintronic devices. Electrodeposition of epitaxial $Fe_3O_4$ films on Ni single crystals is a challenge due to the large +138% mismatch between the lattice parameters of the two materials. However, epitaxial electrodeposition and chemical bath deposition have been demonstrated for large mismatch systems, in which the mismatch can be reduced by the formation of coincidence lattices.[6,7] Here, we report the epitaxial electrodeposition of $Fe_3O_4$ on a Ni(111) single crystal, in which the lattice mismatch is reduced to −0.7% by forming a coincidence lattice. The epitaxial film shows resistance switching at 77 K and a magnetoresistance (MR) of −0.8% at 9 T and 200 K.

$Fe_3O_4$ is a ferrimagnetic mixed-valence 3d transition metal oxide (space group, $Fd\bar{3}m$) with a lattice parameter of 0.8397 nm. $Fe_3O_4$ undergoes a metal-to-insulator Verwey transition at $T_v \approx 120$ K,[8] and the Curie temperature of magnetite is 860 K. Above $T_v$, $Fe_3O_4$ has an inverse-spinel structure with $Fe^{3+}$ occupying tetrahedral sites and $Fe^{3+}$, $Fe^{2+}$ occupying octahedral sites. Electronic conduction at temperatures above $T_v$ has been attributed to hopping of spin-polarized electrons between magnetically ordered $Fe^{3+}$ and $Fe^{2+}$ in octahedral sites. However, below $T_v$, $Fe_3O_4$ undergoes a first-order phase transition to a monoclinic unit cell through charge ordering at octahedral sites.[9−11]

Epitaxial thin films of $Fe_3O_4$ have been grown by MBE, pulsed laser deposition, laser ablation, and oxidation of Fe thin films on a variety of substrates.[11b,12] Our group has previously reported on epitaxial electrodeposition of $Fe_3O_4$ on Au(111), Au(110) and Au(100) single crystals from both acidic and basic solutions.[13] In this work, the cathodic electrodeposition of epitaxial $Fe_3O_4$ films was carried out from an alkaline solution containing 43.3 mM iron(III) sulfate, 100 mM TEA (triethanolamine), and 2 M NaOH (~pH 14). The deposition temperature was 80 °C and the deposition potential was −1.01 V vs Ag/AgCl. The thickness of the film was approximately 300 nm.

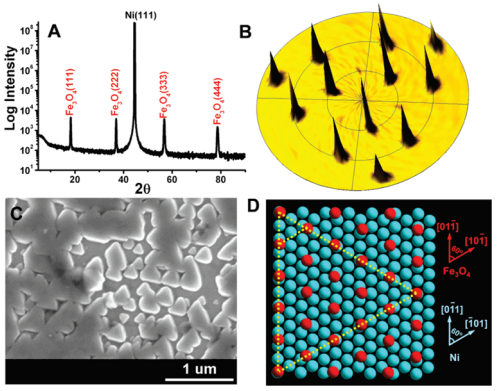


**Figure 1.** (A) X-ray 2$\theta$ scan of the film. Only the {111} family of planes of $Fe_3O_4$ are observed. (B) (311) pole figure of $Fe_3O_4$ on Ni(111), (C) SEM micrograph showing the triangular islands of $Fe_3O_4$ on Ni(111), and (D) an interface model for $Fe_3O_4$(111) on Ni(111). The close-packed Ni atoms are colored light blue, and the O atoms are colored red. The large yellow triangle defines the coincidence lattice which has a mismatch of −0.7%.

The orientation of the $Fe_3O_4$ film grown on single-crystal Ni(111) was determined by X-ray diffraction (XRD) using a high-resolution ($\lambda$ = 1.54056 Å) four-circle diffractometer (Philips X'Pert MRD). The 2$\theta$ scans in Figure 1A probe the out-of-plane orientation of the film. Only the {111} family of peaks of $Fe_3O_4$ are observed. The lattice parameter of 0.8394 nm determined for the $Fe_3O_4$ film agrees well with the known bulk lattice parameter, indicating that the majority of the film is relaxed. The in-plane orientation of the film was determined by X-ray pole figures. Figure 1B shows the (311) pole figure of $Fe_3O_4$ film on the Ni(111) single crystal. The radial grid lines in the pole figure correspond to 30° increments in the tilt angle. The

**Received:** January 21, 2011
**Revised:** March 4, 2011
**Published:** March 29, 2011

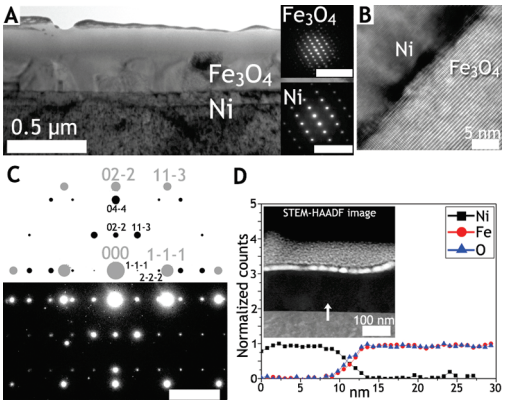


**Figure 2.** (A) Conventional bright-field TEM image showing the sharp interface, insets show the corresponding diffraction patterns (scalebar is 20 $nm^{-1}$). (B) HRTEM image of the $Fe_3O_4$/Ni interface (Image processing: Noise filtered through fast Fourier transformation). (C) The calculated diffraction patterns (rotated by 90° with respect to A) overlay (above) in agreement with experimental selected area diffraction (SAD) pattern of the interface between $Fe_3O_4$ and Ni (below). (the scalebar is 5 $nm^{-1}$). (D) EELS line scan on the $Fe_3O_4$/Ni interface shows that there is no excess oxygen at the interface.

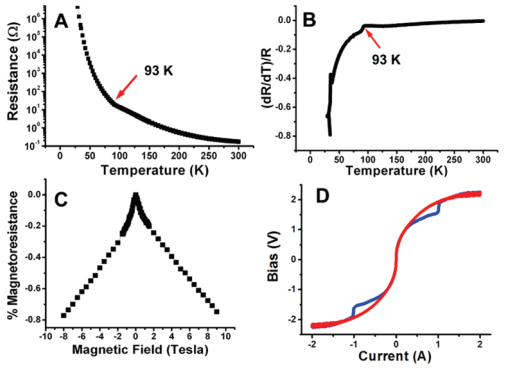


**Figure 3.** (A) Resistance vs temperature curve indicating a Verwey transition at 93 K. (B) Differential plot normalized with resistance which indicates a clear Verwey transition at 93 K. (C) Magnetoresistance plot at 200 K for a $Fe_3O_4$ film deposited on Ni(111). (D) iV curve showing resistance switching, obtained by scanning the applied current at 50 mA/s. Blue line indicates forward sweep and red line indicates backward sweep.

(311) reflections on the pole figure occur at tilt angles, $\chi$, of 29.5, 58.5, and 80°. The epitaxial relationship between the film and substrate was determined from azimuthal scans. The azimuthal scans were obtained by selecting the Ni (311) planes at $2\theta$ = 93.044°, the $Fe_3O_4$ (311) planes at $2\theta$ = 35.456°, and tilting the sample to $\chi$ = 29.5°. The azimuthal scans show that the $Fe_3O_4$ film is rotated by 180° around the [111] axis relative to the Ni substrate, which gives the epitaxial relationship $Fe_3O_4(111)[01\bar{1}]//Ni(111)[0\bar{1}1]$. The 3-fold-symmetric azimuthal scans show that the $Fe_3O_4$ film is 99% oriented antiparallel to the substrate. The SEM image of $Fe_3O_4$ on the Ni(111) single crystal in Figure 1C is consistent with the pole figure analysis. For the SEM micrograph, a region of the film was selected where complete coalescence had not occurred. The micrograph reveals that the majority of the film is dominated by one set of triangular islands of $Fe_3O_4$ terminated by {111} facets. The majority of the facets are aligned in-plane, with a few facets rotated 180°. The interface model in Figure 1D is consistent with the epitaxial relationship determined from the X-ray pole figure. In the interface model, close-packed Ni atoms are colored light blue and O atoms are colored red. The spacing between the adjacent O atoms is 0.5937 nm and the spacing between Ni atoms is 0.2491 nm. By comparing the spacing between oxygen atoms and Ni atoms, the lattice mismatch is calculated to be +138% in the Ni ⟨011⟩ in-plane directions. The mismatch is dramatically lowered to −0.7% when the spacing between 5 unit meshes of O is compared with 12 unit meshes of Ni in the ⟨011⟩ directions.

A cross-section of the $Fe_3O_4$/Ni interface was studied by transmission electron microscopy (TEM). Figure 2A shows a conventional bright-field image of $Fe_3O_4$ grown on Ni, obtained through third order aberration corrected TEM (TITAN$^3$ 80−300, FEI Company) operated at 300 kV. The insets show the selected area diffraction (SAD) patterns of the film and substrate. The SAD patterns of both the film and the substrate indicate a $\langle 2\bar{1}1 \rangle$ orientation of the cross-section and describes a direction lying in the (111) interface plane. This is consistent with the XRD results. Figure 2B shows a high-resolution TEM (HRTEM) image of the interface. The image reveals that the interface between $Fe_3O_4$ and Ni is sharp. Figure 2C shows the SAD pattern obtained from the interface. The pattern shows spots of similar planes from both the film and the substrate. This confirms the epitaxial orientation relationship indicated by XRD. Also, the spot pattern is indexed using an overlay of calculated diffraction patterns, using JEMS software, of $Fe_3O_4$ and Ni. The calculated pattern is in agreement with the experimental spot pattern and further supports the epitaxial nature of the interface. In addition, electron energy loss spectroscopy (EELS) was performed across the interface, as shown in Figure 2D. The scan indicates the absence of any excess oxygen, ruling out the possibility of a NiO layer.

Magnetic measurements were carried out with a Quantum Design Physical Property Measurement System (PPMS) using the resistivity option for the instrument. Perpendicular transport measurements were carried out by making pressure contacts. Two silver wires were attached, one to the $Fe_3O_4$ film and the other to the Ni surface by pressing indium metal. Figure 3A shows the resistance versus temperature plot of the epitaxial $Fe_3O_4$ film electrodeposited on Ni(111). The plot reveals an increase in resistance below 93 K indicating the Verwey transition. Figure 3B displays the differential plot of the resistance versus temperature. The plot shows a dip at 93 K in agreement with Figure 3A, indicative of the Verwey transition temperature. One possible explanation for the shift of the Verwey transition from the bulk value of ∼120 K to a lower temperature is related to nonstoichiometric $Fe_3O_4$ formation as seen by other researchers.[14] We prepare the films by electrochemical reduction of a Fe(III)-TEA (triethanolamine) complex at 80 °C in strongly alkaline solution. The deposition is believed to occur by electrochemical−chemical (EC) mechanism described by eq 1 and 2.

$$Fe(TEA)^{3+} + e^- \rightleftarrows Fe^{2+} + TEA \quad (1)$$

$$Fe^{2+} + 2Fe(TEA)^{3+} + 8OH^- \rightleftarrows Fe_3O_4 + 2TEA + 4H_2O \quad (2)$$

Because of the EC nature of the deposition reaction, it is possible to control the composition of the films through the applied potential.[13d,15] Stoichiometric $Fe_3O_4$ can be produced at −1.05 V vs Ag/AgCl. Material deposited at potentials more positive than −1.05 V have excess Fe(III), and those deposited at potentials more negative than −1.05 V have excess Fe(II).[15]


dx.doi.org/10.1021/cm2002176 |Chem. Mater. 2011, 23, 2017–2019

That would imply that the films grown at −1.01 V would have excess Fe(III), resulting in nonstoichiometric $Fe_3O_4$ film formation. For such films, the Verwey temperature is shifted to a lower value. Whereas for a stochiometric magnetite film grown at −1.05 V vs Ag/AgCl on Ni(111), the Verwey transition temperature is ∼118 K, which is very close to the Verwey transition temperature of bulk $Fe_3O_4$. Films were deposited at −1.01 V vs Ag/AgCl in this study, because the films deposited at −1.05 V were highly twinned. Figure 3C shows the out-of-plane magnetoresistance (MR) scan at 200 K obtained for an electrodeposited $Fe_3O_4$ film on Ni(111). A MR value of −0.8% at 9 T was obtained for the film, similar to what we had previously reported for polycrystalline $Fe_3O_4$.[13c] We had anticipated that a $Fe_3O_4$/NiO/Ni tunneling magnetoresistance (TMR) structure would form, with a thin NiO layer serving as the tunnel barrier in a ferrimagnetic/antiferromagnetic/ferromagnetic sandwich. Similar architectures in metals have shown a giant magnetoresistance effect (GMR).[16] However, the electrodeposited $Fe_3O_4$ films on Ni(111) do not show a TMR or GMR effect. This is consistent with the absence of NiO at the interface as confirmed by our TEM analysis.

A particularly interesting feature that the electrodeposited magnetite films exhibit is resistance switching during perpendicular transport measurements.[15] Recently, we have shown that superlattices in the magnetite system and polycrystalline magnetite films exhibit resistance switching.[15] It was shown that the films with nonstoichiometric $Fe_3O_4$ exhibit both low-to-high and high-to-low jumps.[15b] Figure 3D shows the iV curve obtained at 77 K by sweeping the current from 0 to 2 A at 50 mA/s for a −1.01 V $Fe_3O_4$ film on Ni(111). During the forward scan it is seen that the film undergoes a low-to-high resistance jump at ±1.5 V. Low-to-high resistance switching has previously been reported in $Fe_3O_4$ and the origin of such switching has been attributed to the oxidation of $Fe_3O_4$ to $\gamma$-$Fe_2O_3$ at the anode.[17] We believe that in our case also the low-to-high resistance occurs due to the oxidation of $Fe_3O_4$ to $\gamma$-$Fe_2O_3$ under the contact. As reported before, we do not observe the insulator-to-metal phase transition jump in our epitaxial films.[15] It was shown previously that nanophase magnetite is critical for the phase transition jump to occur.[15,18] Epitaxial magnetite films and single crystals show high-to-low resistance switching (phase transition jump) only at very high bias (∼10 V).[19] Similarly, the epitaxial $Fe_3O_4$ films deposited on the single-crystal Ni(111) do not show the phase transition jump.

In conclusion, we have demonstrated that epitaxial films of $Fe_3O_4$ can be electrodeposited onto a Ni(111) single crystal. The film grows with [111] perpendicular to the sample plane and the in-plane $[01\bar{1}]$ direction of $Fe_3O_4$ aligned with the in-plane $[0\bar{1}1]$ direction of Ni(111). The TEM results are in agreement with XRD results. The EELS line scan shows that there is no NiO interlayer between the electrodeposited $Fe_3O_4$ film and the Ni(111) substrate. The $Fe_3O_4$ film on Ni(111) has a Verwey transition temperature which is shifted to a lower value of 93 K from the bulk value of 120 K. We believe that this shift is due to the nonstoichiometery of $Fe_3O_4$. A magnetoresistance value of −0.8% is obtained at 9 T and 200 K. The films of $Fe_3O_4$ on Ni(111) exhibit high-to-low resistance switching at 77 K.

The authors thank Dr. Eric Bohannan for his useful comments and discussions and Dina Lohse for TEM specimen preparation. The work was supported by Department of Energy Grant DE-FC07−03ID14509.

## AUTHOR INFORMATION

**Corresponding Author**
*E-mail: jswitzer@mst.edu.

## REFERENCES

(1) (a) Zhang, Z.; Satpathy, S. *Phys. Rev. B* **1991**, *44*, 13319. (b) Anisimov, V. I.; Elfimov, I. S.; Hamada, N.; Terakura, K. *Phys. Rev. B* **1996**, *54*, 4387.
(2) Julliere, M. *Phys. Lett.* **1975**, *54A*, 225.
(3) (a) Versluijs, J. J.; Bari, M. A.; Coey, J. M. D. *Phys. Rev. Lett.* **2001**, *87*, 026601. (b) Seneor, P.; Fert, A.; Maurice, J. −L.; Montaigne, F.; Petroff, F.; Vaures, A. *Appl. Phys. Lett.* **1999**, *74*, 4017. (c) Chen, P.; Xing, D. Y.; Du, Y. M.; Zhu, J. M.; Feng, D. *Phys. Rev. Lett.* **2001**, *87*, 107202.
(4) Voogt, F. C.; Palstra, T. T. M.; Niesen, L.; Rogojanu, O. C.; James, M. A.; Hibma, T. *Phys. Rev. B* **1998**, *57*, R8107.
(5) Margulies, T.; Parker, F. T.; Spada, F. E.; Goldman, R. S.; Li, J.; Sinclair, R.; Berkowitz, A. E. *Phys. Rev. B* **1996**, *53*, 9175.
(6) Nakanishi, S.; Lu, G.; Kothari, H. M.; Bohannan, E. W.; Switzer, J. A. *J. Am. Chem. Soc.* **2003**, *123*, 14998.
(7) Mu, G.; Gudavarthy, R. V.; Kulp, E. A.; Switzer, J. A. *Chem. Mater.* **2009**, *21*, 3960.
(8) Verwey, E. J. W. *Nature* **1939**, *144*, 327.
(9) (a) Walz, F. *J. Phys. Condens. Mater.* **2002**, *14*, R285. (b) Gracia, J.; Subias, G. *J. Phys. Condens. Mater* **2004**, *16*, R145.
(10) (a) Huang, D. J.; Lin, H.-J.; Okamoto, J.; Chao, K. S.; Jeng, H.-T.; Guo, G. Y.; Hsu, C.-H.; Huang, C.-M.; Ling, D. C.; Wu, W. B.; Yang, C. S.; Chen, C. T. *Phys. Rev. Lett.* **2006**, *96*, 096401. (b) Nazarenko, E.; Lorenzo, J. E.; Joly, Y.; Hoeau, J. L.; Mannix, D.; Marin, C. *Phys. Rev. Lett.* **2006**, *97*, 056403.
(11) (a) Subias, G.; Gracia, J.; Blasco, J.; Proietti, M. G.; Renevier, H.; Sanchez, M. C. *Phys. Rev. Lett.* **2004**, *93*, 156408. (b) Rozenberg, Kh.; Pasternak, M. P.; Xu, W. M.; Amiel, Y.; Hanfland, M.; Amboage, M.; Taylor, R. D.; Jeanloz, R. *Phys. Rev. Lett.* **2006**, *96*, 045705.
(12) (a) Anderson, F.; Kuhn, M.; Diebold, U.; Shaw, K.; Stoyanov, P.; Lind, D. *Phys. Rev. B* **2002**, *56*, 9902. (b) Gong, G. Q.; Gupta, A.; Xiao, G.; Qian, W.; Dravid, V. P. *Phys. Rev. B* **1997**, *56*, 5096. (c) Kennedy, R. J.; Stampe, P. A. *J. Phys. D: Appl. Phys.* **1999**, *32*, 16. (d) Weiss, W.; Ritter, M. *Phys. Rev. B* **1999**, *59*, 5201.
(13) (a) Nikiforov, M. P.; Vertegel, A. A.; Shumsky, M. G.; Switzer, J. A. *Adv. Mater.* **2000**, *12*, 1351. (b) Sorenson, T. A.; Morton, S. A.; Waddill, G. D.; Switzer, J. A. *J. Am. Chem. Soc.* **2002**, *124*, 7604. (c) Kothari, H. M.; Kulp, E. A.; Limmer, S. J.; Poizot, P.; Bohannan, E. W.; Switzer, J. A. *J. Mater. Res.* **2006**, *21*, 293. (d) Kulp, E. A.; Kothari, H. M.; Limmer, S. J.; Yang, J.; Gudavarthy, R. V.; Bohannan, E. W.; Switzer, J. A. *Chem. Mater.* **2009**, *21*, 5502.
(14) (a) Kakol, X. Z.; Honig, J. M. *Phys. Rev. B* **1989**, *40*, 9090. (b) Shepherd, Y. J. P.; Koenitzer, J. W.; Aragón, R.; Sandberg, C. J.; Honig, J. M. *Phys. Rev. B* **1985**, *31*, 1107.
(15) (a) Switzer, J. A.; Gudavarthy, R. V.; Kulp, E. A.; Mu, G.; He, Z.; Wessel, A. *J. Am. Chem. Soc.* **2010**, *132*, 1258. (b) Gudavarthy, R. V.; Miller, A. S.; Bohannan, E. W.; Kulp, E. A.; He, Z.; Switzer, J. A. *Electrochim. Acta* **2011**In press.
(16) Binasch, G.; Grünberg, P.; Sauernbach, F.; Zinn, W. *Phys. Rev. B* **1989**, *39*, 4828.
(17) Odagawa, A.; Katoh, Y.; Kanzawa, Y.; Wei, Z.; Mikawa, T.; Muraoka, S.; Takagi, T. *Appl. Phys. Lett.* **2007**, *91*, 133503.
(18) Lee, S.; Fursina, A.; Mayo, J. T.; Yavuz, C. T.; Colvin, V. L.; Sofin, R. G. S.; Shevts, I. V.; Natelson, D. *Nat. Mater.* **2008**, *7*, 130.
(19) Burch, T. J.; Craig, P. P.; Hedrick, C.; Kitchens, T. A.; Budnick, J. I.; Cannon, J. A.; Lipsicas, M.; Mattis, D. *Phys. Rev. Lett.* **1969**, *23*, 1444.